

UBVI CCD PHOTOMETRY OF YOUNG OPEN CLUSTERS. II. BOCHUM 7

HWANKYUNG SUNG^{1,5}, M. S. BESSELL², B.-G. PARK^{3,4}, AND Y. H. KANG¹

¹Department of Earth Science Education, Kyungpook National University, Taegu 702-742

²Research School of Astronomy & Astrophysics, Australian National University, Private Bag, Weston Creek, ACT 2611, Australia

³Bohyun-san Optical Astronomy Observatory, Yeongcheon 770-820

⁴Department of Astronomy & Atmospheric Sciences, Kyungpook National University, Taegu 702-742

⁵Present address: Bohyun-san Optical Astronomy Observatory, Yeongcheon 770-820

(Received Sep. 15, 1999; Accepted Sep. 29, 1999)

ABSTRACT

UBVI CCD photometry has been obtained for a region around the Wolf-Rayet star WR 12. We found two young stellar associations in the observed field: the nearer one comprises the field members of Vela OB1 association at $d = 1.8$ kpc, while the farther one is the young open cluster Bochum 7 (Bo 7) at $d = 4.8$ kpc. The stars associated with Bo 7 showed no central concentration which suggests that Bo 7 is not a young open cluster but simply a local concentration in the density of young stars belonging to the OB association (Vel OB3). These two associations have similar ages but remarkably different mass function slopes ($\Gamma = -2.1 \pm 0.3$ for Vel OB1 and -1.0 ± 0.3 for Bo 7). The stars in Vel OB1 shows an evident age spread ($\Delta\tau \sim 9$ Myr). We also found two strong H α emission stars - WR 12 and #1066 - from narrow band H α photometry.

Key words : color-magnitude diagrams (H-R diagram) - open clusters and associations: individual (Bo 7) - stars : early-type - initial mass function(IMF)

I. INTRODUCTION

The Vela region of the Milky Way is an interesting region for understanding the spiral structure of the Galaxy. Vela is located in the inter-arm region between the inner Sgr-Car arm and the local (Cyg-Ori) arm. Several surveys searching for southern luminous stars (LSS catalog - Stephenson & Sanduleak 1971) or young open clusters (Moffat & Vogt 1975) found many young OB stars in the region. The existence of a young population in the interarm region stimulated many follow-up observations (Muzzio 1979; Muzzio & Orsatti 1977; Bassino et al. 1982; Eggen 1986; Slawson & Reed 1988; Reed & Slawson 1990). This region is known as the Vela "spur".

In her compilation of luminous stars, Humphreys (1978) listed only one OB association (Vel OB1 at 1.8 kpc) in Vela. However we now believe that there are at least three OB associations in Vela, with suggestions for a fourth at 1 kpc and a fifth at 110 pc. Moffat & Vogt (1974) observed several OB stars from the LSS catalog in the Vela region and found a young stellar group (Bo 7) at 5.8 kpc ($V_0 - M_V = 13.8 \pm 0.6$). They suggested that the young stars around WR 12 may also be an OB association (known as Vel OB3).

The existence of nearer OB associations was proposed as early as 1914 by Kapteyn. The reality of Vel OB2 and its distance were debated for a long time (for details, see de Zeeuw et al. 1999), but recently de Zeeuw et al. (1999) confirmed its existence at 410 ± 12 pc using *Hipparcos* parallax and proper motion data. γ^2 Vel - the nearest known WR star and one of the

important stars for calibrating the absolute magnitude scale of WR stars, - was confirmed as a member of Vel OB2. From a study of the stellar population at $(l, b) = (268, 0)$ in Vela, Slawson & Reed (1988) and Reed & Slawson (1990) found another OB star population at 1.0 ± 0.1 kpc and proposed it as the fourth OB association in Vela (Vel OB4). More recently Tovmassian et al. (1993) found a nearby B association at 110 pc from the analysis of UV data obtained from the "Glazar" space telescope.

This is the second paper on the systematic observational study of young open clusters. In the first paper (Sung & Lee 1995 - Paper I) we discussed the initial mass function (IMF) and age spread in the young open cluster IC 1805 in Cassiopeia. In Paper I we obtained a very flat IMF and a spread in age for low mass stars. Young open clusters and OB associations are very important objects for understanding the underlying star formation processes as well as studying the spiral structure of the Galaxy. Bo 7, more precisely Vel OB3, is a distant young open cluster (or OB association) and can give some information on the spiral structure of the outer region. Lundström & Stenholm (1984) obtained the distance $y_0 \approx 13.5$ to the region, which is slightly smaller than that derived by Moffat & Vogt (1975).

In this paper we will present new UBVI CCD photometry for one region around WR star CD -45° 4482 (= WR 12 = MR 13 = LSS 1145). Observation and data reduction procedures will be summarized in Section II. From these data, we will show the existence of two distinct groups of OB stars in the observed re-

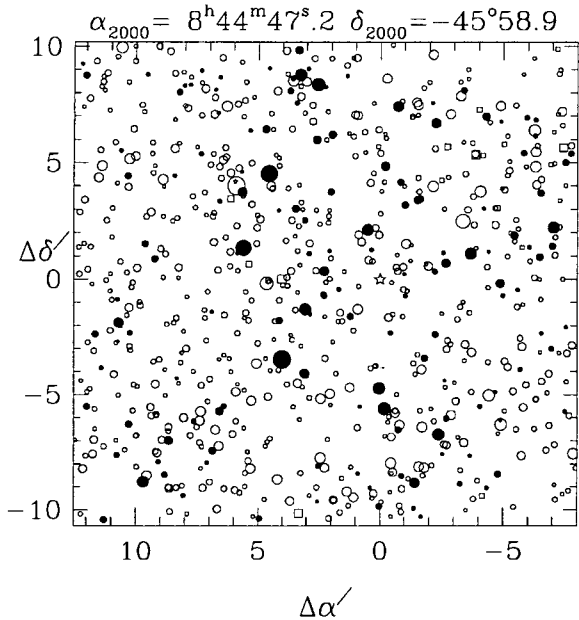


Fig. 1.— Finding chart, centered at $\alpha = 8^h 44^m 47^s.2$, $\delta = -45^\circ 58.9$ (J2000.0). The size of the symbol is proportional to the magnitude of the star. Filled circles, squares, stars and open circles represent respectively stars belonging to Vel OB1, to Bo 7 (Vel OB3), H α emission stars and field stars. See Section III(b) for membership selection criteria.

gion in Section III. Several fundamental parameters for these two populations will be derived in the same section. In Section IV, we construct the physical HR diagram and by overlaying the theoretical stellar and pre-main sequence (PMS) tracks, we estimate the age and age spread of these two young stellar populations and derive the IMFs. Section V contains the discussion of the results, especially the slope of IMF. Section VI is the summary.

II. OBSERVATIONS

UBVI CCD photometry for the region was performed on 1997 March 4 using the 1m telescope (f/8) at Siding Spring Observatory. During that observing run we observed SA 98 and PG 1323-086 as standard regions (Landolt 1992). Later we found some problems in the transformation of *U* (see equation (4) of Sung et al. 1998; see also Sung & Bessell 1999b). To transform *U* magnitudes properly to the Landolt standard system, we should know the reddening of individual stars. For early type stars ($Sp < B5$) the reddening can be calculated easily, but individual reddenings for late type stars are very difficult to determine due to metallicity and gravity effects on ($U - B$).

In order to avoid systematic errors in ($U - B$), we re-observed the same region on 1999, February 5 and used for the *U* observations an additional UG2 1mm

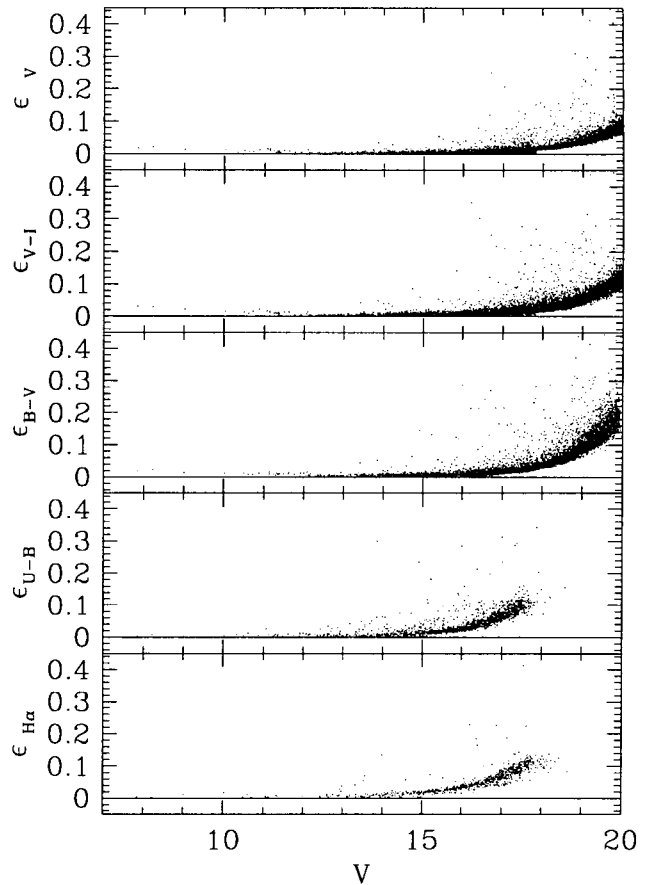


Fig. 2.— Photometric errors in magnitude and color against *V* magnitude.

filter to minimize the non-linear transformation term. In addition, we observed SAAO E region standards (E3 and E5). We also obtained narrow band H α images and continuum images to search for H α emission stars. The main reason for using a narrow band H α and continuum filters is to achieve a better resolution (Lee & Sung 1998). The central wavelength and bandwidth of H α and continuum filters are (H α : $\lambda_0 = 6563\text{\AA}$, $\Delta\lambda = 15\text{\AA}$, continuum filter : $\lambda_0 = 6676\text{\AA}$, $\Delta\lambda = 35\text{\AA}$). Mean extinction coefficients were applied ($k_{1V} = 0.161$, $k_{1B} = 0.308$, $k_{2B} = 0.031$, $k_{1U} = 0.537$, $k_{2U} = 0.013$, $k_{1I} = 0.088$, $k_{1H\alpha} = 0.092$, $k_{1C} = 0.089$). We obtained images for two sets of exposure times: long, 60^s in *I*, 150^s in *V*, 300^s in *B* and continuum, 600^s in *U*, 3 \times 600^s in H α ; and short, 5^s in *V* and *I*, 10^s in *B*, 20^s in continuum, 60^s in *U*. The transformation relations used here are

$$V = v - k_{1V}X + 0.072(B - V) + \zeta_V, \quad (1)$$

$$V = v - k_{1V}X + 0.074(V - I) + \zeta'_V, (V - I \leq 1.5) \quad (2)$$

$$V = v - k_{1V}X + \zeta''_V, (V - I > 1.5) \quad (3)$$

Table 1. Photometric data^a

ID	$\Delta\alpha(^{\circ})^b$	$\Delta\delta(^{\circ})^b$	V	$V-I$	$B-V$	$U-B$	$H\alpha$	ϵ_V	ϵ_{V-I}	ϵ_{B-V}	ϵ_{U-B}	$\epsilon_{H\alpha}$	n_{obs}				Sp	Remark	
316	-3.358	2.486	10.025	1.975	1.835	2.204	1.073	0.012	0.016	0.013	0.006	0.018	1	1	1	2	2		
547	-0.174	-5.612	10.616	0.157	0.108	-0.446	1.240	0.007	0.010	0.008	0.013	0.012	2	2	1	1	2	WN7	WR12, LS1145
562	0.000	0.000	10.726	1.098	0.570	-0.314	-0.012	0.007	0.015	0.007	0.003	0.003	1	1	1	2	1		
566	0.035	-4.719	11.068	0.160	0.126	-0.321	1.310	0.016	0.016	0.016	0.002	0.006	2	2	1	1	2		
723	2.558	8.356	10.332	0.263	0.204	-0.459	...	0.005	0.011	0.008	0.008	...	1	1	1	1	1		
772	3.266	8.774	10.871	0.380	0.250	-0.301	...	0.012	0.023	0.012	0.006	...	1	1	1	1	1		
868	4.558	4.525	8.221	0.308	0.194	-0.447	1.089	0.022	0.029	0.023	0.008	0.003	1	1	1	1	1	B4II	HD74936, LS1149
877	4.649	-0.177	10.497	0.601	0.542	0.021	1.213	0.011	0.014	0.013	0.006	0.004	1	1	1	1	2		
942	5.598	1.350	9.014	0.135	0.109	-0.579	1.153	0.013	0.023	0.014	0.005	0.011	1	1	1	1	2	B4II	CD-45 4501, MM2
967	5.908	4.012	7.861	0.180	0.178	0.174	1.387	0.018	0.032	0.019	0.005	0.004	1	1	1	1	1		

^a This is a sample of the full table, which is available from HS.

^b Relative to WR star CD -45° 4482 ($\alpha_c = 8^h 44^m 47.^s 2$, $\delta_c = -45^\circ 58.'9$, J2000.0).

$$B = b - [k_{1B} - 0.031(B - V)]X - 0.101(B - V) + \zeta_B, \quad (4)$$

$$U = u - [k_{1U} - 0.013(U - B)]X + 0.125(U - B) + \zeta_U, \quad (U - B \leq 0.0) \quad (5)$$

$$U = u - [k_{1U} - 0.013(U - B)]X + 0.006(U - B) + \zeta_U, \quad (U - B > 0.0) \quad (6)$$

$$I = i - k_{1I}X + 0.028(V - I) + \zeta_I. \quad (7)$$

More detailed discussion relating to the transformation will be discussed elsewhere (Sung & Bessell 1999b). All other procedures, such as pre-processing and point spread function fitting photometry, are the same as before (see Sung et al. 1998).

Photometric data for 1,423 stars brighter than $V = 17$ mag are presented in Table 1. Table 1 lists the running number, $\Delta\alpha(^{\circ})$, $\Delta\delta(^{\circ})$ relative to WR star CD -45° 4482, the weighted mean values of the magnitude and colors, their errors and number of independent measurements. The spectral type and other names are listed in the last two columns. (Table 1 is available from HS.) Fig. 1 is the finding chart for stars brighter than $V = 16$ mag from this study and an additional bright star (HD 74920) from photoelectric photometry by previous investigators. The size of the symbol is proportional to the magnitude of the star. Filled circles, squares, stars and open circles represent respectively stars belonging to Vel OB1, to Bo 7 (Vel OB3), $H\alpha$ emission stars, and field stars. The errors in magnitude and color are shown plotted against V magnitude in Fig. 2. We compared our new results for 7 stars brighter than $V = 14$ mag in common with Miller & McCarthy (1974). The mean difference (photoelectric - CCD) and standard deviation in V , $(B - V)$, and $(U - B)$ are $+0.016$ (± 0.043), $+0.002$ (± 0.023), and -0.039 (± 0.033), respectively.

III. PHOTOMETRIC DIAGRAMS AND MEMBERSHIP SELECTION

(a) Reddening and Distance

We present color-color diagrams from our photometry in Fig. 3. We also included in Fig. 3(a) the brightest star in the observed region (HD 74920) and two evolved supergiant stars (HD 75149 and HD 75276) to the east of the observed field. In the $(U - B)$ versus $(B - V)$ diagram, there are two young stellar groups with different mean reddening. The range of reddening of each group is marked in the figure. Bo 7 is located near the center of the Vel OB1 association and therefore we can expect low mass members of Vel OB1 to be in the observed region. The less reddened stars are the members of Vel OB1, while the more reddened stars are the stars belonging to more distant Bo 7 (Vel OB3).

The interstellar reddening $E(B - V)$ can be determined by comparing $(B - V)$ and $(U - B)$ colors with the intrinsic color-color relation of Mermilliod (1981). The scatter in the color-color diagrams can be easily interpreted as differential reddening across the observed field. The range of reddening $E(B - V)$ for Vel OB1 is $0.20 \sim 0.45$, while that of Bo 7 is $0.75 \sim 1.05$. From photographic photometry and spectral classification using objective prism plates for the $(l, b) = (268, 0)$ region, Reed & Slawson (1990) found a sharp increase in $E(B - V)$ from 0.24 mag to 1.06 mag at $d = 0.85 \sim 1.6$ kpc. The reddening for the Vel OB1 stars in our observed region ($l \sim 265^\circ$, $b \sim -2^\circ$) does not show such an increase in reddening [*i.e.* the “Vela sheet” (Eggen 1986) does not exist in the observed region] and the amount of reddening is also far lower. The amount of reddening for Bo 7 is very similar to that obtained by Moffat & Vogt (1975, $E(B - V) = 0.86 \pm 0.13$).

The differential reddening map derived from individual early type stars belonging to each group was drawn in Fig. 4. The north-western region of Vel OB1 is more obscured, while the south-eastern region is less reddened. The spatial variation of the reddening for Bo 7 is slightly different from that for Vel OB1, although the reddening for Bo 7 is somewhat uncertain due to the small number of early type members belonging to the association.

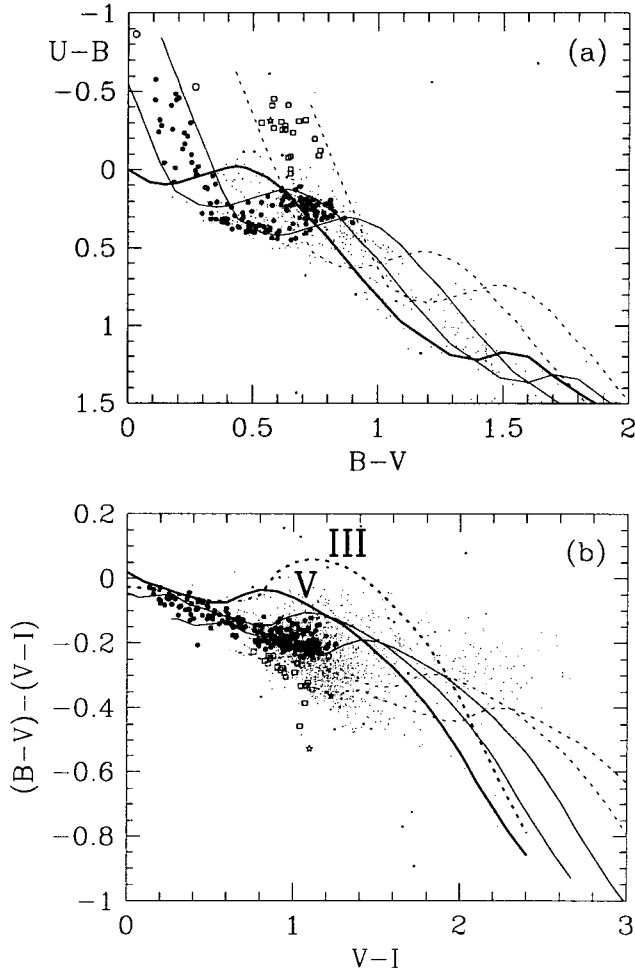


Fig. 3.— Color-color diagrams. The thick solid line represents the ZAMS relation, two thin solid lines represent the reddened ZAMS relations for Vel OB1 with $E(B-V)_{min}^{Vel\ OB1}$ and with $E(B-V)_{max}^{Vel\ OB1}$, and two dotted lines represent the reddened ZAMS relations for Bo 7 with $E(B-V)_{min}^{Bo\ 7}$ and with $E(B-V)_{max}^{Bo\ 7}$. The open circle represents bright Vel OB1 members from photoelectric photometry of previous investigators. The thick dotted line in (b) denotes the unreddened relation for giants. The other symbols (filled circles, squares and star marks) are the same as Fig. 1.

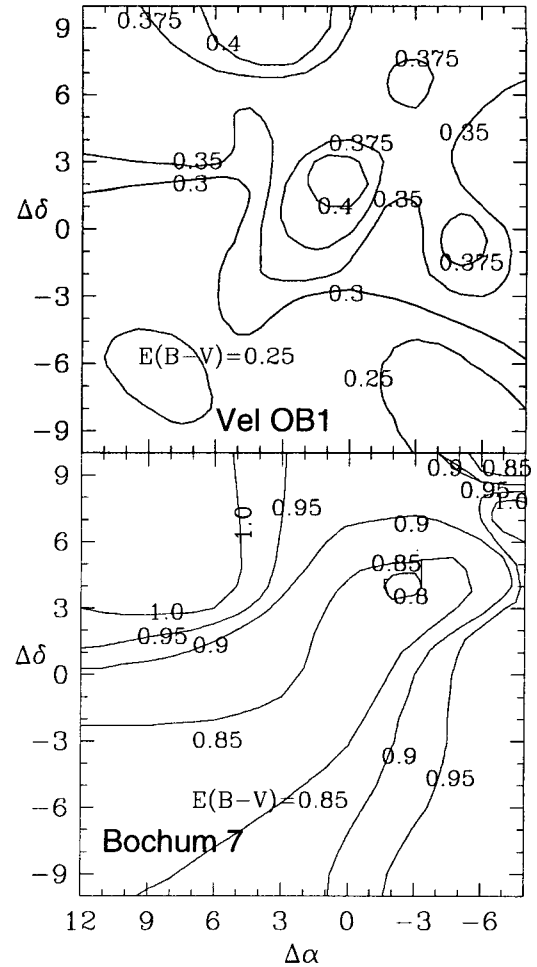


Fig. 4.— Differential reddening map. The numbers indicated are interstellar reddening $E(B-V)$.

To determine the distance to the cluster, we should know the ratio of total to selective extinction, R [$\equiv A_V/E(B-V)$]. The R -value is related to the color-excess ratio as $R = 2.45 E(V-I)/E(B-V)$ (Guetter & Vrba 1989). The reddening in $(V-I)$ for early-type stars is calculated by using $(B-V)/(V-I)$ relation of Sung & Bessell (1999a). For Vel OB1 stars, the scatter in $E(V-I)/E(B-V)$ is very large (1.12~1.39) probably due to the small value of $E(B-V)$ and intrinsic scatter in $(V-I)_0$. For Bo 7, the mean value of $E(V-I)/E(B-V)$ is 1.343 ± 0.019 from 14 early-type stars. This means that the R -value for Bo 7 is 3.29 ± 0.05 . We adopt $R = 3.3 \pm 0.1$ both for Vel OB1 and Bo7. WR 12 shows a very large value [$E(V-I)/E(B-V) \approx 1.675$] implying an IR excess of the star. This star also shows strong $H\alpha$ emission as expected for usual WR stars.

Using the ZAMS relation of Mermilliod (1981) and Sung & Bessell (1999a), the distance modulus of indi-

vidual stars can be calculated. The distribution of distance moduli of stars in Vel OB1 shows a broad peak at $V_0 - M_V = 11.1 \sim 11.5$ mag indicating the association nature of the group. We adopted the distance modulus of Vel OB1 as $V_0 - M_V = 11.3 \pm 0.2$ mag ($d = 1.8 \pm 0.2$ kpc). This value is well consistent with values obtained by Humphreys (1978, $V_0 - M_V = 11.3$ mag) and Tovmassian et al. ($d = 1.7 \pm 0.15$ kpc). For Bo 7, the determination of a distance modulus is very difficult due to the small number of early-type members. However, 6 stars amongst 17 stars with $(B - V)_0 < 0.2$ have $(V_0 - M_V) = 13.39 \pm 0.05$ mag. The other stars have smaller values probably due both to the evolution effect and the effect of unresolved companions. We adopted the distance modulus of the association as $(V_0 - M_V) = 13.4 \pm 0.1$ mag ($d = 4.8 \pm 0.2$ kpc). This value is slightly smaller than that obtained by Moffat & Vogt (1975: $[V_0 - M_V] = 13.8 \pm 0.6$ mag) but larger than that determined from one star by Tovmassian et al. (1993: $d = 4$ kpc).

(b) Membership Selection

The membership criteria for early-type stars are relatively simple and straightforward, *i.e.* reddening and distance, and applied the same way as in our previous papers (see Paper I or Sung et al. 1997, 1998). The brightest star in the observed region, HD 74920 (O7III : Reed & Beatty 1995), was not included in the Vel OB1 member list by Humphreys (1978), but its distance and reddening suggest that it is a Vel OB1 member so we have included it. For late B type stars, membership assignment is a very difficult problem due to contamination by less reddened foreground stars. The contamination by foreground field stars can be easily seen in the color-magnitude diagrams in Fig. 5.

Recently Sung & Bessell (1999a) applied a new membership selection criterion to the nearby intermediate age open cluster M35. They used the difference in reddening effect on the colors $B - V$ and $V - I$. After correcting for reddening using the differential reddening map in Fig. 4, the distance modulus of an individual star was estimated using the $(V - I, M_V)$ and $(B - V, M_V)$ relations. Ideally, members of each association should give the same value for the distance modulus for both colors, but the photometric errors and the existence of an unresolved companion affect the colors differently. Sung & Bessell (1999a) considered a star to be a member if the mean value of its distance modulus is consistent with the cluster value. (Actually to take into account the effect of an unresolved companion, they considered a range of mean values of distance modulus up to equal mass binary, *i.e.* $[V_0 - M_V]_{cl} + 2\sigma_{V_0 - M_V} \sim [V_0 - M_V]_{cl} - 0.75 - \sigma_{V_0 - M_V}$) and the difference in distance moduli is less than 0.25 mag ($2.5\sigma_{V_0 - M_V}$).

The photometric membership criterion mentioned above has some limitations. For distant clusters or associations, the differences in reddening and distance modulus between cluster stars and field stars are very

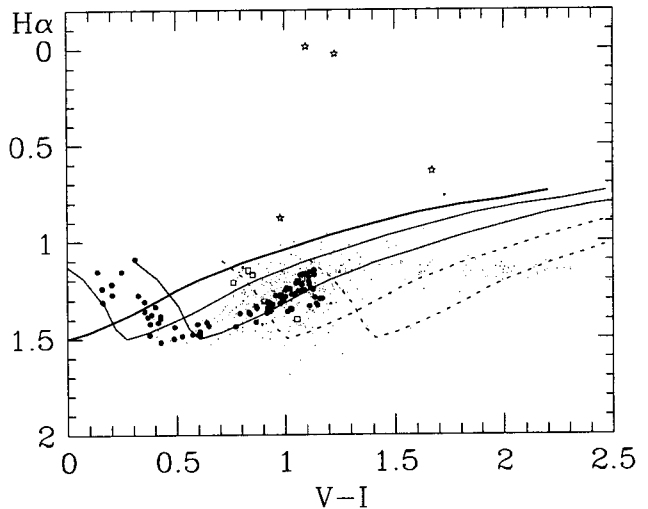


Fig. 6.— $H\alpha$ versus $(V - I)$ diagram. The uppermost thick solid line represents the reddening-corrected MS relation from the observations of NGC 2353. The two thin solid lines denote reddened $[E(B - V)_{min}^{Vel OB1}$ and $E(B - V)_{max}^{Vel OB1}]$ MS relations for Vel OB1, while the two dotted lines are those for Bo 7. The other symbols are the same as Fig. 3.

small, and therefore the contamination by field stars is inevitable for late type stars. Such a contamination by field stars is severe for Vel OB1 because there are many F-, G-type foreground field stars in the observed region. But for Bo 7, contamination by field stars is less severe because all the members of Bo 7 are B- or earlier type stars. To reduce the contamination by field stars to Vel OB1, further restrictions were applied. Firstly, for bright stars ($V < 16.5$), *i.e.* stars having relatively reliable $(U - B)$, we used the $(B - V, U - B)$ diagram. We only selected stars between the minimum and maximum reddening lines.

Secondly, we used an $H\alpha$ index ($\equiv H\alpha - C$) as in Fig. 6. The small number of stars detected by $H\alpha$ photometry was due to the narrow bandwidth of the $H\alpha$ filter and by vignetting beyond $7'$ from the image center. Two strong $H\alpha$ emission stars (WR12 & #1066) and two weak $H\alpha$ emission stars (#867 & #969) were found. Their photometric values are listed in Table 2. It is very difficult to decide to which group these three $H\alpha$ emission stars belong. But as Muzzio (1979) found that most of the $H\alpha$ emission stars (with only one exception) belong to the distant group, we therefore temporarily assign these $H\alpha$ emission stars to Bo 7 (= Vel OB3). With regard to the Vel OB1 stars, we selected stars with an $H\alpha$ index between the minimum and maximum reddening lines, but lowered the weight to take into account relatively large errors in the $H\alpha$ photometry.

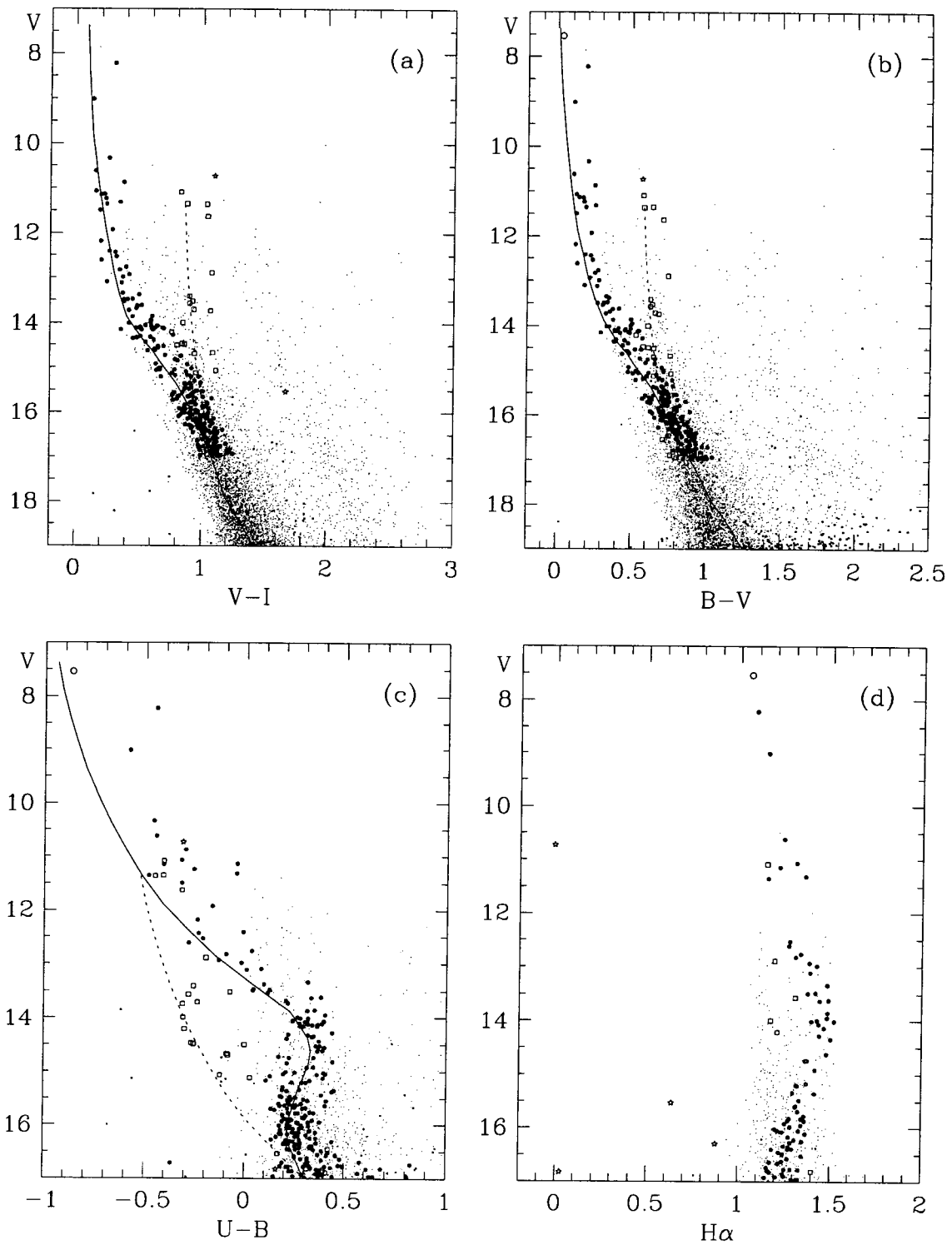


Fig. 5.— Color-magnitude diagrams. The solid lines represent the reddened ZAMS relation for Vel OB1 applying the median value of reddening and adopted distance modulus. The dotted lines represent that for Bo 7. The $H\alpha$ index is defined by the color ($H\alpha - C(\text{continuum})$). The other symbols are the same as Fig. 3.

Table 2. H α emission stars

ID	$\Delta\alpha(^{\circ})$	$\Delta\delta(^{\circ})$	V	$V-I$	$B-V$	$U-B$	$H\alpha$	ϵ_V	ϵ_{V-I}	ϵ_{B-V}	ϵ_{U-B}	$\epsilon_{H\alpha}$	n_{obs}	Sp	Remark
562	0.000	0.000	10.726	1.098	0.570	-0.314	-0.012	0.007	0.015	0.007	0.003	0.003	1 1 1 2 1	WN7	WR12,LS1145
1066	7.154	1.073	16.824	1.229	0.866	0.160	0.027	0.018	0.020	0.022	0.048	0.041	2 2 1 1 1		
867	4.507	4.299	16.293	0.979	0.783	...	0.877	0.023	0.034	0.035	...	0.059	2 2 1 1		
969	5.943	4.190	15.531	1.672	0.636	0.015	0.015	0.064	2 2 1		

Table 3. Mass function

log m	N	log $\xi(\log m)^a$	log m	N	log $\xi(\log m)$
Vela OB1 Association					
1.0 ~ 1.6 ...	1	4.151	0.9 ~ 1.6 ...	1	4.084
0.8 ~ 1.0 ...	1	4.628	0.7 ~ 0.9 ...	2	4.929
0.6 ~ 0.8 ...	4	5.230	0.5 ~ 0.7 ...	7	5.473
0.4 ~ 0.6 ...	11	5.669	0.3 ~ 0.5 ^b ...	20	5.929
0.2 ~ 0.4 ^b ...	54	6.360	0.1 ~ 0.3 ^b ...	119	6.704
0.0 ~ 0.2 ^b ...	166	6.848			
Bochum 7 (Vel OB3)					
1.1 ~ 1.5 ...	4	4.089	1.2 ~ 1.5 ...	4	4.214
0.9 ~ 1.0 ...	5	4.487	1.0 ~ 1.2 ...	4	4.390
0.7 ~ 0.9 ...	8	4.691	0.8 ~ 1.0 ...	6	4.566
0.5 ~ 0.7 ...	8	4.691	0.6 ~ 0.8 ...	5	4.487
0.3 ~ 0.5 ...	18	5.043	0.4 ~ 0.6 ...	19	5.067

IV. HERTZSPRUNG-RUSSELL DIAGRAM

(a) Age and Age Spread

To obtain the observational HR diagram, it is necessary to transform the observational quantities into physical parameters. We used the adopted calibrations given in Sung et al. (1998) and constructed the HR diagrams for Vel OB1 and Bo 7 shown in Fig. 7. The stellar evolution models by Schaller et al. (1992) and the PMS evolution models by Bernasconi & Maeder (1996) are superimposed. Several isochrones interpolated from these evolution models are overlaid in the figure. Filled circles represent stars in Vel OB1, while squares denote stars belonging to Bo 7 (Vel OB3). We also included two nearby Vel OB1 members (HD 75149 & HD 75276) in the figure to better derive an age spread in Vel OB1. As they are evolved supergiants they can give better ages. The spectral type of WR star CD -45° 4482 is WN7 and the derivation of its physical quantities is outside our adopted calibrations. Its position in Fig. 7 was obtained by assuming that it is a normal O7II star ($\log T_{eff} = 4.271$, BC = -2.05 mag). If we take into account the observational and theoretical comparison by Smith et al. (1994), the BC scale of WR12 is about -4.0 mag ($M_{bol} = -9.4$ mag). The position of WR12 in the HR diagram is consistent with the enhanced mass loss tracks of Meynet et al. (1994, see their Fig 4) within the uncertainty of the temperature calibration of WR stars.

The age of these two stellar populations can be estimated from the isochrones plotted in the figure. The mean age of each group has a similar value ($\tau_{age} = 6$ Myr) but Bo 7 shows scarcely any spread in age, while Vel OB1 shows a somewhat large spread in age. The brightest star in the observed field, HD 74920 (O7III),

is well positioned on the isochrone of age 3.5 Myr, while one of nearest evolved supergiant HD 75276 (F2Iab) is well fitted to the isochrone of age 12.5 Myr. The age spread of Vel OB1, therefore, is about 9 Myr. This value is somewhat large relative to the value obtained from observations of other young open clusters (Massey et al. 1995; Paper I; Sung et al. 1998).

(b) Initial Mass Function

The masses of individual stars were determined by using stellar evolution models (Schaller et al. 1992) or PMS evolution models (Bernasconi & Maeder 1996). From these, the number of stars in logarithmic mass intervals (initial mass function: IMF) of $\Delta \log m = 0.2$ for $\log m \leq 1.0$ were derived. For massive stars ($\log m > 1.0$) the whole range of mass was considered. The IMF $\xi(\log m)$ is defined by the number of stars born in unit logarithmic mass per unit area in kpc^2 . We also calculated the number of stars in the same bin size, but shifted by 0.1 in $\log m$ to smooth out the binning effect. The calculated IMFs are listed in Table 3 and shown in Fig. 8. The mass of the most massive normal star in Bo 7 is $\sim 25M_{\odot}$. The initial mass of the WR star CD -45° 4482 may have been more massive than $25M_{\odot}$. The cutoff mass at $\tau_{age} = 6$ Myr is about $30M_{\odot}$ from the stellar evolution models with high mass loss during MS and WNL phase (Meynet et al. 1994). We took this star as the most massive star in Bo 7 and included it in the highest mass bin in the IMF calculation.

We also derived the slope of the IMF, $\Gamma (\equiv d \log \xi / d \log m)$ for $\log m > 0.4$ to minimize the effect of the field star contamination. Massey et al. (1995) obtained $\Gamma = -1.1 \pm 0.1$ for stars with masses $> 7M_{\odot}$ from the observations of young open clusters as well as

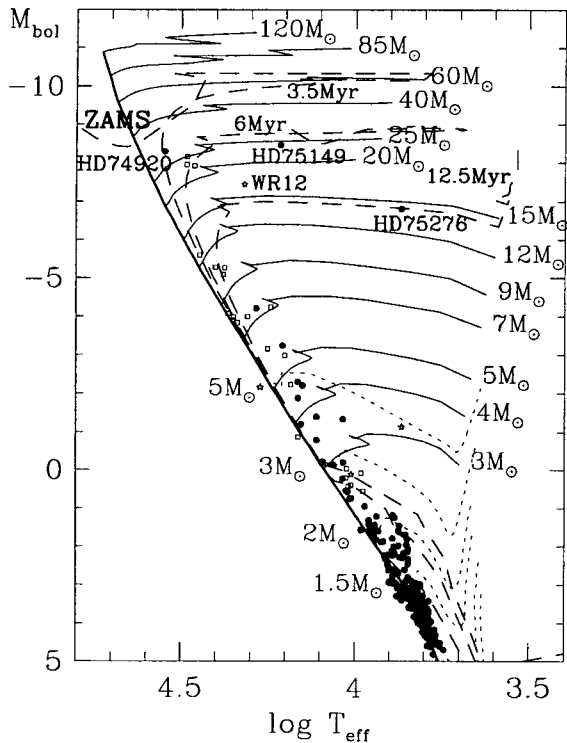


Fig. 7.— H-R diagram. The thick solid line represents the ZAMS of Schaller et al. (1992). The thin solid lines with mass to the right are the stellar evolution models of Schaller et al., while the dotted lines with mass to the left are the PMS evolutionary tracks by Bernasconi & Meader (1996). The long dashed lines represent isochrones. The other symbols are the same as Fig. 3.

OB associations in the Galaxy and Magellanic Clouds. However the two OB associations we observed have far different IMF slopes. Vel OB1 has a very steep IMF, while Bo 7 shows a very normal IMF slope.

V. DISCUSSION

(a) IMF Slope

We derived the IMF of Vel OB1 and of Bo 7 in Section IV(b) and obtained very different IMF slopes for them. This could be a real effect or it could be an artifact due to contamination of field stars in the Vel OB1 association or to insufficient spatial sampling. We applied several membership criteria in selecting members for each association; but the main criterion using the distance moduli and reddening characteristics cannot be a good criterion for clusters or associations at large distance and/or having no distinct reddening differences between members and field stars. Vel OB1 is relatively less affected by interstellar reddening. In addition, several investigators proposed the existence of another OB association at about 1 kpc (Slawson & Reed 1988; Tovmassian et al. 1993). Even though we

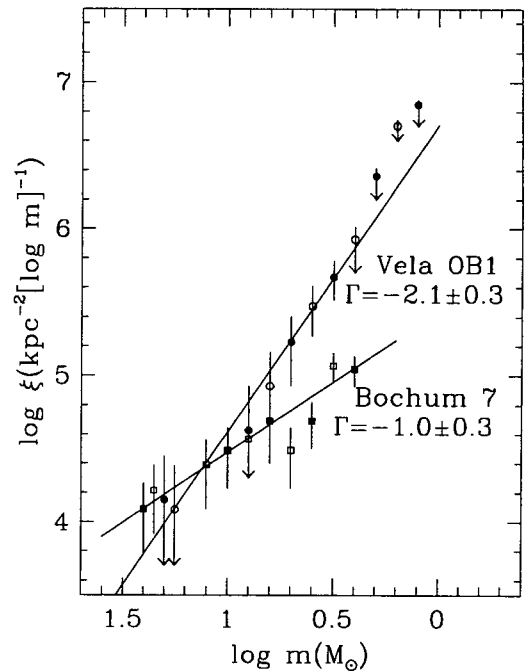


Fig. 8.— Initial mass function. Circles and squares represent the IMF of Vel OB1 and Bo 7, respectively. Open and filled symbols represent respectively the IMF binned in 0.2 in $\log m$, but shifted by 0.1 in $\log m$. The error bars are based on $N^{1/2}$. The down arrows at $\log m < 0.5$ represent the upper limit due to the contamination of field stars.

could find no firm evidence as to the existence of an association at 1 kpc, the possibility cannot be excluded that they may be included as binary members of the Vel OB1 association. To exclude such a contamination, we used $(U - B, B - V)$ as well as $(H\alpha, V - I)$ color-color diagrams, but for the fainter stars the quality of $(U - B)$ and $H\alpha$ were not good enough.

Could the apparent difference in the IMF slope be real? Massey et al. (1995) observed many young open clusters and OB associations in the Milky Way as well as in the Magellanic Clouds. They found a diverse range of IMF slopes ($\Gamma = -0.7 \sim -2.1$, see their table 5) although they concluded that there was no significant difference in IMF slopes (the average value is $\Gamma = -1.1 \pm 0.1$).

Theoretical support for differing slopes in the IMF has come from recent work by Silk (1995) who derived a semi-empirical relation between slope of the IMF and the line widths in molecular cores by supposing that the core line widths, which are predominantly non-thermal, originate from high-velocity protostellar outflows. He interpreted the difference in IMF slope as resulting from protostellar wind characteristics and the density structure of the core. For a highly time-variable outflow or a relatively uniform density, as in the center of a

cloud, the IMF is flat, while for a decaying wind or radiatively expanding bubble it is steep. His picture is very difficult to apply to associations because an association is the site of large-scale star formation processes and therefore individual wind characteristics may not affect the IMF of the association although it could affect subgroups within the association.

More observations are required to check whether the difference in IMF slope is a real feature or an artifact due to small spatial coverage or to the inclusion of field stars.

VI. SUMMARY

UBVI CCD photometric data has been obtained for a region, formerly known as the young open cluster Bo 7, in Vela. The results obtained are summarized as follows.

(i) We identified two OB associations in the observed region. The less reddened foreground stars are members of Vel OB1, while the more reddened background stars are members of Bo 7, *i.e.* Vel OB3.

(ii) The distance and range of reddening $E(B - V)$ of the associations are 11.3 ± 0.2 mag ($d = 1.8 \pm 0.2$ kpc) and $0.20 \sim 0.45$ mag respectively for Vel OB1, and 13.4 ± 0.1 mag ($d = 4.8 \pm 0.2$ kpc) and $0.75 \sim 1.05$ mag respectively for Bo 7.

(iii) The ages of two associations was derived by using the stellar evolution models of the Geneva group. These two associations have similar ages ($\tau_{age} \approx 6$ Myr). Vel OB1 shows evident age spread about 9 Myr, while Bo 7 shows little spread in age.

(iv) The IMFs were derived for the associations. The IMF slope of Bo 7 is normal ($\Gamma = -1.0 \pm 0.3$), while that of Vel OB1 is very steep ($\Gamma = -2.1 \pm 0.3$). Discussions relating to the IMF slopes were presented.

(v) Two strong $H\alpha$ emission stars, WR 12 & #1066, and two weak $H\alpha$ emission stars were found from narrow band $H\alpha$ photometry.

H.S. acknowledges the support of the Kyungpook National University's Post-Doc Program. H.S. would like to express his thanks to Department of Astronomy & Atmospheric Sciences, Kyungpook National University for the use of their computer facilities.

REFERENCES

- Bassino, L. P., Dessaunet, V. H., Muzzio, J. C., & Waldhausen, S. 1982, MNRAS, 201, 885
- Bernasconi, P. A., & Maeder, A. 1996, A&A, 307, 829
- Eggen, O. J. 1986, AJ, 92, 1074
- Guetter, H. H., & Vrba, F. J. 1989, AJ, 98, 611
- Humphreys, R. M. 1978, ApJS, 38, 309
- Landolt, A. U. 1992, AJ, 104, 340
- Lee, K. H., & Sung, H. 1998, JKAS, 31, 101
- Lundström, I., & Stenholm, B. 1984, A&AS, 58, 163
- Massey, P., Johnson, K. E., & Degioia-Eastwood, K. 1995, ApJ, 454, 151
- Mermilliod, J.-C. 1981, A&A, 97, 235
- Meynet, G., Maeder, A., Schaller, G., Schaerer, D., & Charbonnel, C. 1994, A&AS, 103, 97
- Miller, E. W., & McCarthy, C. C. 1974, AJ, 79, 1294
- Moffat, A. F. J., & Vogt, N. 1975, A&AS, 20, 85
- Muzzio, J. C. 1979, AJ, 84, 639
- Muzzio, J. C., & Orsatti, A. M. 1977, AJ, 82, 474
- Reed, B. C., & Beatty, A. E. 1995, ApJS, 97, 189
- Reed, B. C., & Slawson, R. W. 1990, AJ, 100, 156
- Schaller, G., Schaerer, D., Meynet, G., & Maeder, A. 1992, A&AS, 96, 269
- Silk, J. 1995, ApJ, 438, L41
- Slawson, R. W., & Reed, B. C. 1988, AJ, 96, 988
- Smith, L. F., Meynet, G., & Mermilliod, J.-C. 1994, A&A, 287, 835
- Stephenson, C. B., & Sanuleak, N. 1971, Warner and Swasey Obs., 1, No. 1.
- Sung, H., & Bessell, M. S. 1999a, MNRAS, 306, 361
- Sung, H., & Bessell, M. S. 1999b, Pub. of Ast. Soc. of Australia, submitted
- Sung, H., & Lee, S.-W. 1995, JKAS, 28, 119 (Paper I)
- Sung, H., Bessell, M. S., & Lee, S.-W. 1997, AJ, 114, 2644
- Sung, H., Bessell, M. S., & Lee, S.-W. 1998, AJ, 115, 734
- Tovmassian, H. M., Hovhannessian, R. Kh., Epremian, R. A., & Huguenin, D. 1993, A&AS, 100, 501
- de Zeeuw, Hoogerwerf, R., de Bruijne, J. H. J., Brown, A. G. A., & Blaauw, A. 1999, AJ, 117, 354